# Impact of Oxidative Stress and Peroxisome Proliferator–Activated Receptor γ Coactivator-1α in Hepatic Insulin Resistance

**Naoki Kumashiro,[1] Yoshifumi Tamura,[1] Toyoyoshi Uchida,[1] Takeshi Ogihara,[1] Yoshio Fujitani,[1,2] Takahisa Hirose,[1,2] Hideki Mochizuki,[3] Ryuzo Kawamori,[1,2] and Hirotaka Watada[1]**

**OBJECTIVE—**Recent studies identified accumulation of reactive oxygen species (ROS) as a common pathway causing insulin resistance. However, whether and how the reduction of ROS levels improves insulin resistance remains to be elucidated. The present study was designed to define this mechanism.

**RESEARCH DESIGN AND METHODS—**We investigated the effect of overexpression of superoxide dismutase (SOD)1 in liver of obese diabetic model (*db/db*) mice by adenoviral injection.

**RESULTS—***db/db* mice had high ROS levels in liver. Overexpression of SOD1 in liver of *db/db* mice reduced hepatic ROS and blood glucose level. These changes were accompanied by improvement in insulin resistance and reduction of hepatic gene expression of phosphoenol-pyruvate carboxykinase and peroxisome proliferator–activated receptor γ coactivator-1α (PGC-1α), which is the main regulator of gluconeogenic genes. The inhibition of hepatic insulin resistance was accompanied by attenuation of phosphorylation of cAMP-responsive element-binding protein (CREB), which is a main regulator of PGC-1α expression, and attenuation of Jun $NH_2$-terminal kinase (JNK) phosphorylation. Simultaneously, overexpression of SOD1 in *db/db* mice enhanced the inactivation of forkhead box class O1, another regulator of PGC-1α expression, without the changes of insulin-induced Akt phosphorylation in liver. In hepatocyte cell lines, ROS induced phosphorylation of JNK and CREB, and the latter, together with PGC-1α expression, was inhibited by a JNK inhibitor.

**CONCLUSIONS—**Our results indicate that the reduction of ROS is a potential therapeutic target of liver insulin resistance, at least partly by the reduced expression of PGC-1α. ***Diabetes* 57: 2083–2091, 2008**

Accumulation of reactive oxygen species (ROS) plays a critical role in the pathogenesis of various diseases. ROS are generated by the electron transport chain in mitochondrial respiration and are thus increased in conditions associated with enhanced oxidation of energy substrate such as glucose and free fatty acids. Furthermore, ROS is produced by NADPH oxidase, which is activated by various cytokines. The state of insulin resistance is accompanied by increases in the levels of blood glucose, free fatty acids, and adipocytokines and is thus regarded as a state of increased exposure to ROS (1,2). Although the exact mechanism of insulin resistance is not fully understood, recent data implicate ROS in the pathogenesis of multiple forms of insulin resistance (3–5). However, there is little or no information on how ROS induce insulin resistance in vivo.

The tissue ROS level in each organ depends on the production and elimination of ROS. Superoxide dismutases (SODs) are major antioxidant enzymes that degrade superoxide into hydrogen peroxide. At present, three distinct isoforms of SOD have been identified in mammals (6). SOD1, or CuZn-SOD, is a copper- and zinc-containing homodimer. Although this enzyme had been regarded to be expressed exclusively in the cytoplasm, at least in rodent liver, it is found both in the intermembrane space of mitochondria and in the cytosol (7). SOD2, or Mn-SOD, is a manganese-containing enzyme found almost exclusively in the mitochondria. SOD3, or EC-SOD, is the most recently characterized SOD; it exists as a copper- and zinc-containing tetramer and contains a signal peptide that directs this enzyme exclusively to extracellular spaces.

The present study was designed to explore the effect of ROS on hepatic insulin resistance. For this purpose, we injected an adenovirus encoding human SOD1 (AdSOD1) into *db/db* mice, a genetic model of type 2 diabetes. The results demonstrated that reduction of ROS in liver improved glucose tolerance with reduced expression of gluconeogenic genes. The reduced expression of peroxisome proliferator–activated receptor γ coactivator-1α (PGC-1α), independent of insulin signaling at the Akt phosphorylation level, seems to be involved in this mechanism.

## RESEARCH DESIGN AND METHODS

**Recombinant adenoviral vectors.** The recombinant adenovirus AdSOD1 encoding human SOD1 was kindly provided by Dr. David A. Brenner (University of North Carolina) (8). The control adenovirus encoding β-galactosidase (AdLacZ) was kindly provided by Dr. Michael S. German (University of California San Francisco). Both adenoviruses were amplified in human embryonic kidney (HEK)-293 cells and purified by cesium chloride density centrifugation. Viral titers were determined by the method of tissue culture infective doses 50.

**Animals and administration of recombinant adenovirus.** The study was reviewed and approved by the animal care and use committee of Juntendo University. Specific-pathogen–free female C57BL/KsJ-*db/db* mice and their lean littermates, C57BL/KsJ-*db/m* mice, were purchased from Japan Clea (Tokyo, Japan). All mice were housed in stainless steel wire cages in a temperature-controlled clean room with a 12:12 h light-dark cycle. The animals were provided with standard diet and autoclaved tap water ad libitum. AdSOD1 or AdLacZ ($5 \times 10^7$ plaque-forming units) diluted in PBS buffer or the

From the [1]Department of Medicine, Metabolism, and Endocrinology, Juntendo University School of Medicine, Tokyo, Japan; the [2]Center for Therapeutic Innovations in Diabetes, Juntendo University School of Medicine, Tokyo, Japan; and the [3]Department of Neurology, Juntendo University School of Medicine, Tokyo, Japan.

Corresponding author: Hirotaka Watada, hwatada@med.juntendo.ac.jp.

Received 1 February 2008 and accepted 12 May 2008.

Published ahead of print at http://diabetes.diabetesjournals.org on 16 May 2008. DOI: 10.2337/db08-0144.

same volume of PBS alone was injected through the tail vein of 12- to 18-week-old *db/db* mice, whose fasting blood glucose values had reached ~180 mg/dl. Blood samples were collected from the tail vein to measure blood glucose and insulin concentrations. Mice were sacrificed under anesthesia induced by intraperitoneal injection of sodium pentobarbital (50 mg/kg) (Nembutal; Abbott Laboratories, Abbott Park, IL).

**Visualization of intracellular superoxide.** The oxidation-dependent fluorescent dye dihydroethidium (DHE) (Sigma Chemical, St. Louis, MO) was used to evaluate in situ production of superoxide (9). Unfixed frozen livers were cut into 5-μm-thick sections, which were placed on glass slides. Twenty micromolars of DHE were applied to the surface of each tissue section, and the slides were incubated in a light-protected humid chamber at 37°C for 30 min. Images were obtained with a microscope (DXM1200; Nikon, Tokyo, Japan) equipped with a krypton/argon laser. Laser and power settings were identical during acquisition of images of various specimens. Fluorescence was detected with a 585-nm-long pass filter.

**Laboratory tests.** Blood glucose concentrations were measured by a portable glucose meter using the One Touch Ultra (LifeScan, Milpitas, CA). Plasma insulin was measured using an insulin ELISA kit (Morinaga, Takamatsu, Japan).

**Nitrotyrosine assay.** Nitrotyrosine was measured with a nitrotyrosine ELISA kit (OxisResearch, Foster City, CA) (10) using whole-cell extracts of each liver.

**Intraperitoneal glucose tolerance, insulin tolerance, and pyruvate challenge tests.** At 5 days after adenovirus infection, mice were injected intraperitoneally with glucose (0.5 g/kg body wt), regular insulin (2 units/kg body wt) (Humulin; Eli Lilly, Indianapolis, IN), or pyruvate (1.5 g/kg body wt), as previously described (11); blood glucose and serum insulin levels were subsequently measured as described above.

**Immunoprecipitation assay and Western blot analysis.** To determine the tissue distribution of SOD1 expression, various tissues were isolated at 7 days after infection with the adenovirus. To investigate the effect of adenovirus injection, after overnight fasting, the livers were isolated, weighed, and snap-frozen in liquid nitrogen. Some livers were collected at 5 min after injection of 0.5 units regular insulin through inferior vena cava. The isolated tissues were then homogenized by a handheld homogenizer in radioimmunoprotein assay buffer (12). The samples were sonicated on ice and centrifuged at 15,000*g* at 4°C for 30 min. The supernatants were collected and Western blotting analysis was performed as previously described (13). For the immunoprecipitation assay, the isolated tissues were homogenized in radioimmunoprotein assay buffer and immunoprecipitation was conducted by incubating supernatant containing the same amount of protein with the indicated antibody and protein G sepharose for 1 hour at 4°C (12). Anti–CuZn-SOD antibody, anti–PGC-1α antibody, and anti-forkhead transcription factor (FKHR) (H-128) antibody were purchased from Santa Cruz Biotechnology (Santa Cruz, CA). Anti–insulin receptor substrate (IRS)-1 antibody, anti–phospho-IRS-1(Ser$^{307}$) antibody, anti–IRS-2 antibody, anti-phosphotyrosine, clone 4G10 antibody, anti–phosphatidylinositol 3 (PI3)-kinase p85 antibody, and anti-Akt1/protein kinase B-α antibody were obtained from Upstate Biotechnology (Lake Placid, NY). Anti-phosphoAkt (Ser$^{473}$) antibody, anti–cAMP-responsive element-binding protein (CREB) antibody, anti-phospho-CREB (Ser$^{133}$) antibody, anti-p44/p42 (extracellular signal–related kinase [ERK]) antibody, anti–phospho-ERK (Thr$^{202}$/Tyr$^{204}$) antibody, anti–phospho-FKHR (Ser$^{256}$) antibody, anti-p38 antibody, anti–phospho-p38 (Thr$^{180}$/Tyr$^{182}$) antibody, anti–stress-activated protein kinase (SAPK)/JNK antibody, and anti–phospho-SAPK/JNK (Thr$^{183}$/Tyr $^{185}$) antibody were obtained from Cell Signaling Technology (Beverly, MA). Horseradish peroxidase–conjugated anti-rabbit and anti-mouse antibodies were purchased from Bio-Rad Laboratories (Tokyo, Japan).

**Isolation of tissue RNA and real-time quantitative RT-PCR.** Total RNA was extracted from livers by using TRIzol reagent (Invitrogen, Carlsbad, CA). cDNAs were then synthesized using Superscript III RNase H Reverse Transcriptase (Invitrogen) and oligo-dT primers. The resulting cDNAs were amplified using SYBR Green PCR kit (Applied Biosystems, Foster City, CA). Quantitative PCR was performed on an ABI PRISM 7700 sequence detection system (Perkin Elmer Life Sciences, Boston, MA). The relative abundance of mRNAs was calculated by the comparative cycle of threshold ($C_T$) method with TATA box–binding protein mRNA as the invariant control. The primer sequences for mouse PGC-1α, phosphoenol-pyruvate carboxykinase (PEPCK), glucose-6-phosphatase (G6Pase), and glucokinase were previously shown (11). The following primers were also used: TATA box–binding protein (mouse) forward CTCAGTTACAGGTGGCAGCA and reverse ACCAACAATC ACCAACAGCA, IRS-2 (mouse) forward CAGCTATTGGGACCACCACT and reverse GTAGTTCAGGTCGCCTCTGC, PGC-1α (human) forward CCTGCAT GAGTGTGTGCTCT and reverse GCAAAGAGGCTGGTCTTCAC, and TATA box–binding protein (human) forward CGGCTGTTTAACTTCGCTTC and reverse TTCTTGGCAAACCAGAAACC.

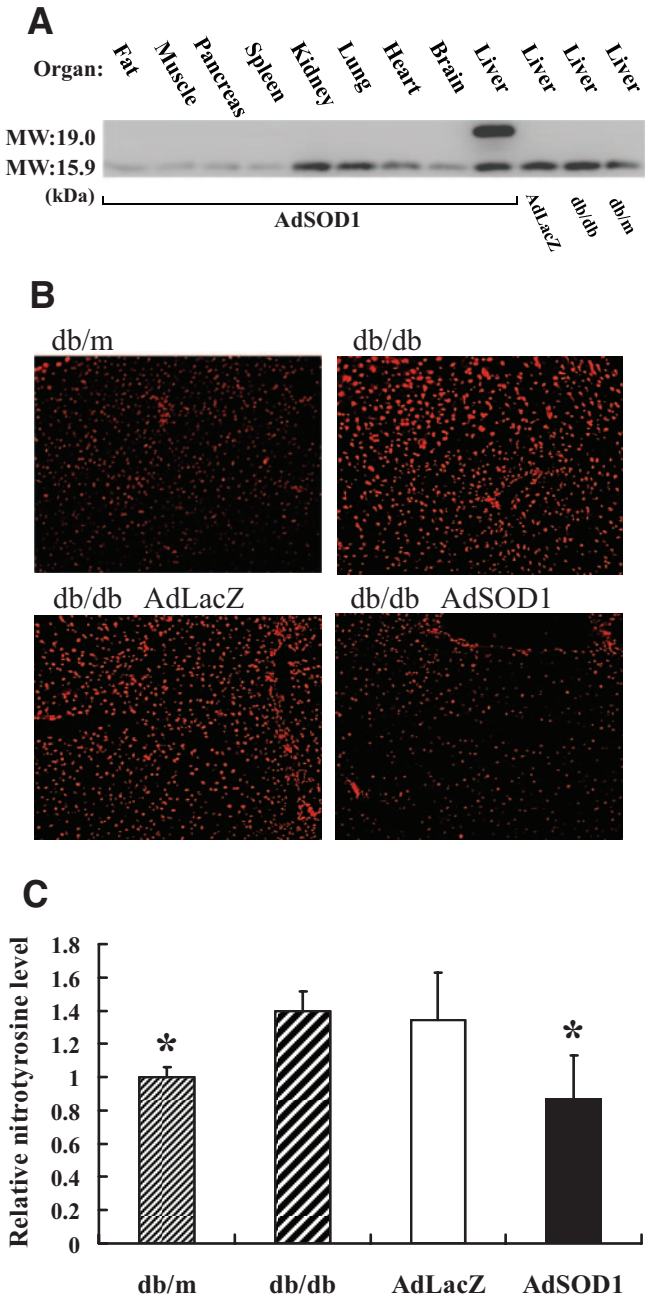


**FIG. 1. Expression of SOD1 and quantification of ROS after injection of AdSOD1 in *db/db* mice. *A*: Seven days after intravenous injection of AdSOD1 ($5 \times 10^7$ plaque-forming units each) into *db/db* mice, each organ was harvested and 20 μg of tissue extracts were immunoblotted with tissue extracts from the liver of AdLacZ-infected *db/db* mice and PBS-injected *db/db* and *db/m* mice using anti-SOD1 antibody. The 19.0-kDa band represents human SOD1 coded in AdSOD1, and the 15.9-kDa band represents endogenous mouse SOD1. *B*: Seven days after the injection of PBS into db/m mice or *db/db* mice or injection of AdLacZ or AdSOD1 into *db/db* mice, the amount of ROS in the liver was visualized by DHE staining. *C*: Quantitative analysis of nitrotyrosine in the liver at 7 days after adenovirus or PBS injection by ELISA. The acquired data by ELISA were corrected for the protein concentration in each sample (*db/m*, $n = 4$; *db/db*, $n = 6$; AdLacZ-treated *db/db*, $n = 10$; and AdSOD1-treated *db/db*, $n = 10$). The relative expression level was expressed by setting the expression level in the *db/m* as 1. Values are expressed as means ± SD. *$P < 0.05$ vs. *db/db* and AdLacZ groups. (Please see http://dx.doi.org/10.2337/db08-0144 for a high-quality digital representation of this figure.)**

**Cell culture.** Human Huh7 hepatocarcinoma cells were kindly provided by Dr. Kenichi Ikejima (Juntendo University, Tokyo). We cultured Huh7 cells in high-glucose Dulbecco's modified Eagle's medium supplemented with 10%

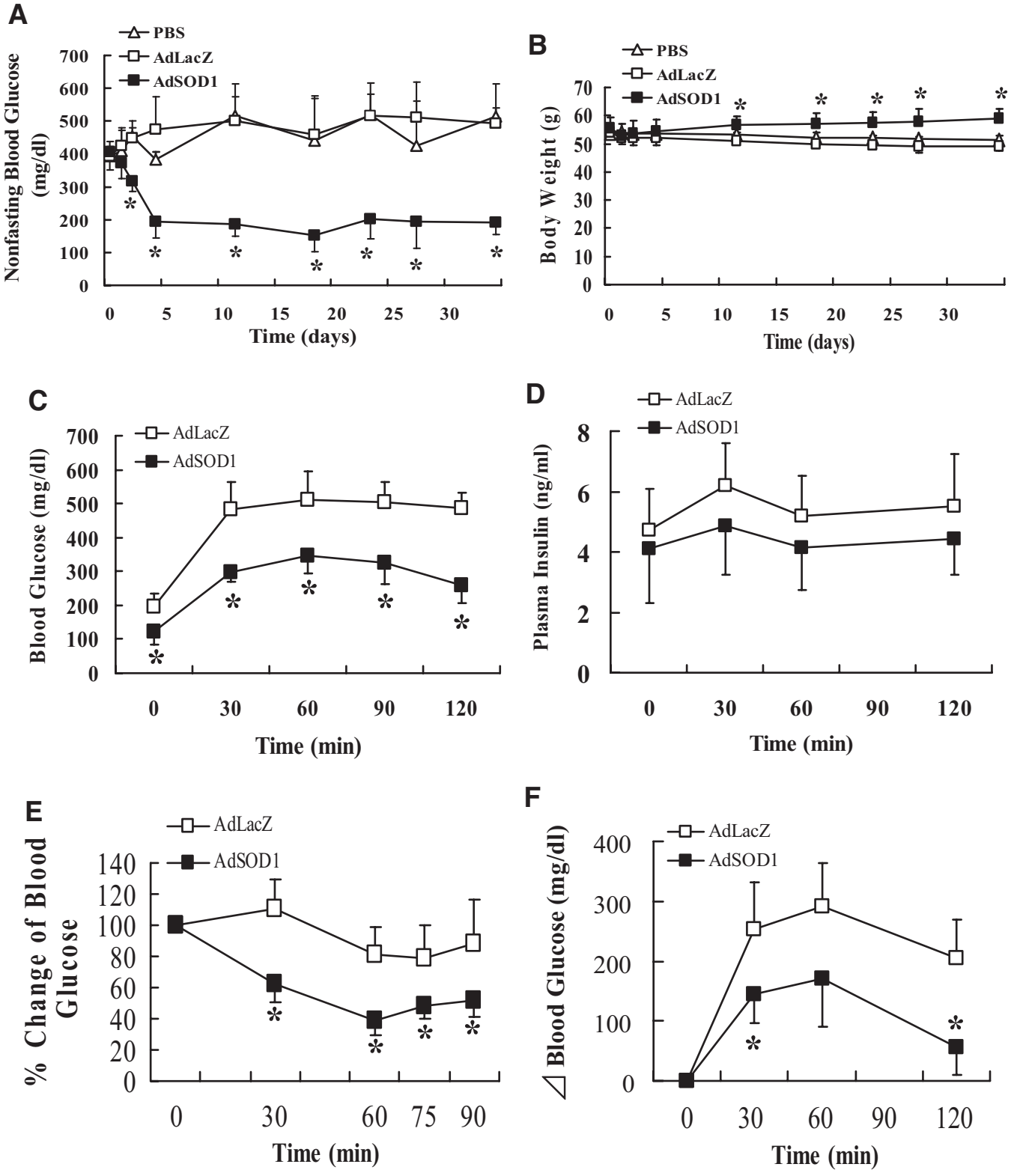


**FIG. 2. Effect of overexpression of AdSOD1 in liver on various metabolic parameters. Serial changes in nonfasting blood glucose level (*A*) and body weight (*B*) after injection of AdSOD1, AdLacZ, or PBS into *db/db* mice ($n = 3$ for each group). Blood glucose (*C*) and immunoreactive insulin concentrations (*D*) after intraperitoneal injection of glucose (0.5 g/kg) at 5 days after each treatment (AdLacZ group, $n = 7$; AdSOD1 group, $n = 6$). *E*: Blood glucose changes (% change) after intraperitoneal injection of 2 units/kg body wt of regular insulin (Humulin) at 5 days after each treatment. Values were calculated by setting the starting blood glucose concentration in each group as 100% ($n = 5$ for each group). *F*: Five days after each treatment, blood glucose concentrations were measured following intraperitoneal pyruvate injection (1.5 g/kg) after overnight fasting ($n = 5$ for each group) as an index of the extent of gluconeogenesis. Values are expressed as means ± SD. *$P < 0.05$ vs. AdLacZ and PBS groups.**

FCS, 100 units/ml penicillin, and 100 μg/ml streptomycin at 37°C in a humidified 5% $CO_2$ environment. To load ROS, Huh7 cells were grown to confluence on six-well plates, incubated overnight in serum-free low-glucose Dulbecco's modified Eagle's medium, and then treated with 400 μmol/l xanthine and 40 mU/ml xanthine oxidase (Sigma) for the indicated time. For analysis of the antioxidant effect, cells were treated with 400 μmol/l butylated hydroxyanisole (BHA) (Sigma) (14,15) or 400 μmol/l manganese (III) tetrakis (4-benzoicacid) porphyrin (MnTBAP) (A.G. Scientific, San Diego, CA) (3) 20

min before the addition of xanthine and xanthine oxidase load. After treatment for the indicated time, cells were washed with PBS and harvested with a scraper. Protein samples or RNA samples were prepared from the lysates and applied for Western blotting or real-time PCR, respectively. In some experiments, we used SP600125 (Calbiochem, San Diego, CA), which is a specific inhibitor of JNK.

**Statistical analysis.** Results are expressed as means ± SD. Differences between two groups were analyzed for statistical significance by Student's *t* test for unpaired comparisons. Comparisons among more than two groups were assessed with ANOVA, followed by a Bonferroni test. A $P$ value $<0.05$ was considered statistically significant.

## RESULTS

**AdSOD1 treatment reduces hepatic ROS in *db/db* mice.** To investigate the effect of reduction of ROS in liver on insulin resistance, we overexpressed SOD1 protein in liver of *db/db* mice by tail-vein injection of AdSOD1, followed by determination of SOD1 gene expression in various organs. Although the expression level of endogenous SOD1 (estimated molecular weight 15.9 kDa) in the liver of *db/db* mice was not less than that in *db/m* mice, endogenous SOD1 was expressed in every organ investigated. On the other hand, exogenous human SOD1 (estimated molecular weight 19.0 kDa) was detected only in AdSOD1-treated liver (Fig. 1*A*). To investigate the effect of SOD1 expression on ROS level in the liver, we stained each liver with the oxidation-dependent fluorescent dye DHE. Hepatic overexpression of SOD1 was associated with reduced level of superoxide in liver to a level comparable with that in *db/m* mice (Fig. 1*B*). This effect was persistently observed from 1 to at least 7 days after the injection of AdSOD1 (data not shown). Nitrotyrosine, a representative marker of protein oxidation in liver of *db/db* mice, was higher than in *db/m* mice. Injection of AdSOD1 into *db/db* mice significantly reduced nitrotyrosine level to a level comparable with that in *db/m* mice, whereas injection of AdLacZ into *db/db* mice did not alter nitrotyrosine level (Fig. 1*C*). These results show that AdSOD1 treatment reduced the increased ROS in the liver of *db/db* mice to a level compatible with that of *db/m* mice.

**Hepatic expression of SOD1 ameliorates glucose intolerance in *db/db mice*.** To elucidate the effect of the reduction of hepatic ROS on glucose metabolism, we investigated the effect of SOD1 overexpression in liver on blood glucose level in *db/db* mice. As shown in Fig. 2*A*, treatment with AdSOD1 induced marked reduction of nonfasting blood glucose level from 2 days after AdSOD1 injection, and this effect continued for at least 33 days. Body weight of AdSOD1-treated mice was higher than that of AdLacZ- mice and PBS-injected control mice (Fig. 2*B*). We measured food intake in each group. Food intake of AdSOD1-treated mice was comparable with that of AdLacZ-treated and PBS-treated mice (data not shown). Accordingly, the increase in body weight in AdSOD1-treated mice was independent of food intake. Intraperitoneal glucose tolerance test revealed that AdSOD1 treatment ameliorated glucose tolerance without an increase in serum insulin level during glucose load (Fig. 2*C* and *D*). Intraperitoneal insulin tolerance test revealed that AdSOD1-treated mice had better insulin sensitivity than AdLacZ-treated mice (Fig. 2*E*). To confirm that the improvement of insulin resistance was mainly due to changes in hepatic glucose metabolism, we measured blood glucose levels after intraperitoneal injection of pyruvate, which is the main precursor of gluconeogenesis. The increase in blood glucose level after pyruvate injection was significantly lower in AdSOD1-treated mice than in AdLacZ-treated mice (Fig. 2*F*). These data indicate that hepatic overexpression of SOD1 improved glucose tolerance mainly by improvement of insulin sensitivity, thus reducing blood glucose level. The reduction of hepatic gluconeogenesis might be at least partly involved in the mechanism.

Steatosis may partly play a causal role in obesity-induced insulin resistance. We investigated the effect of SOD1 expression on hepatic lipid accumulation by Oil Red O staining. The overexpression of SOD1 increased lipid accumulation in liver of *db/db* mice (data not shown). Thus, the improvement of insulin sensitivity in this model is independent of the change of steatosis.

**SOD1 expression in liver reduces PGC-1α expression.** To investigate the mechanism of improvement of hepatic insulin sensitivity by overexpression of SOD1, we measured the mRNA expression of the main regulators of glucose metabolism in the liver by quantitative real-time PCR. Overexpression of SOD1 significantly reduced the expression levels of *PEPCK*, the rate-limiting enzyme of gluconeogenesis. It also modestly reduced the expression level of *G6Pase*, although the effect was not statistically significant. These changes in the expression of gluconeo-

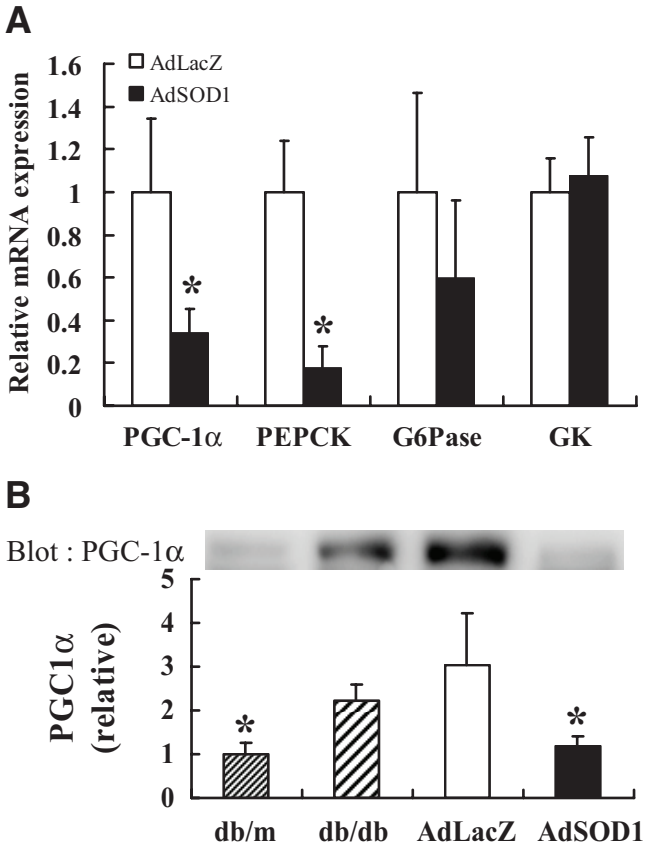


**FIG. 3. Gene expression levels of key metabolic regulators and PGC-1α protein expression in liver overexpressing SOD1. At 7 days after injection of AdLacZ or AdSOD1 into *db/db* mice, livers were collected after overnight fasting. *A*: Total RNA was isolated from the liver of each mouse at fasting state. The mRNA expression levels of key metabolic regulators were measured by real-time RT-PCR. Data were corrected by the expression level of TATA box–binding protein. The relative expression level was calculated by setting the expression level in the liver of mice injected with AdLacZ as 1. Values are means ± SD of 5–6 experiments. *$P < 0.05$ vs. AdLacZ group. *B*: The liver homogenates were immunoblotted with anti–PGC-1α antibody. The relative expression level was calculated by setting the expression level in the liver of db/m mice as 1. Values are means ± SD of 4 experiments. *$P < 0.05$ vs. *db/db*and AdLacZ groups.**

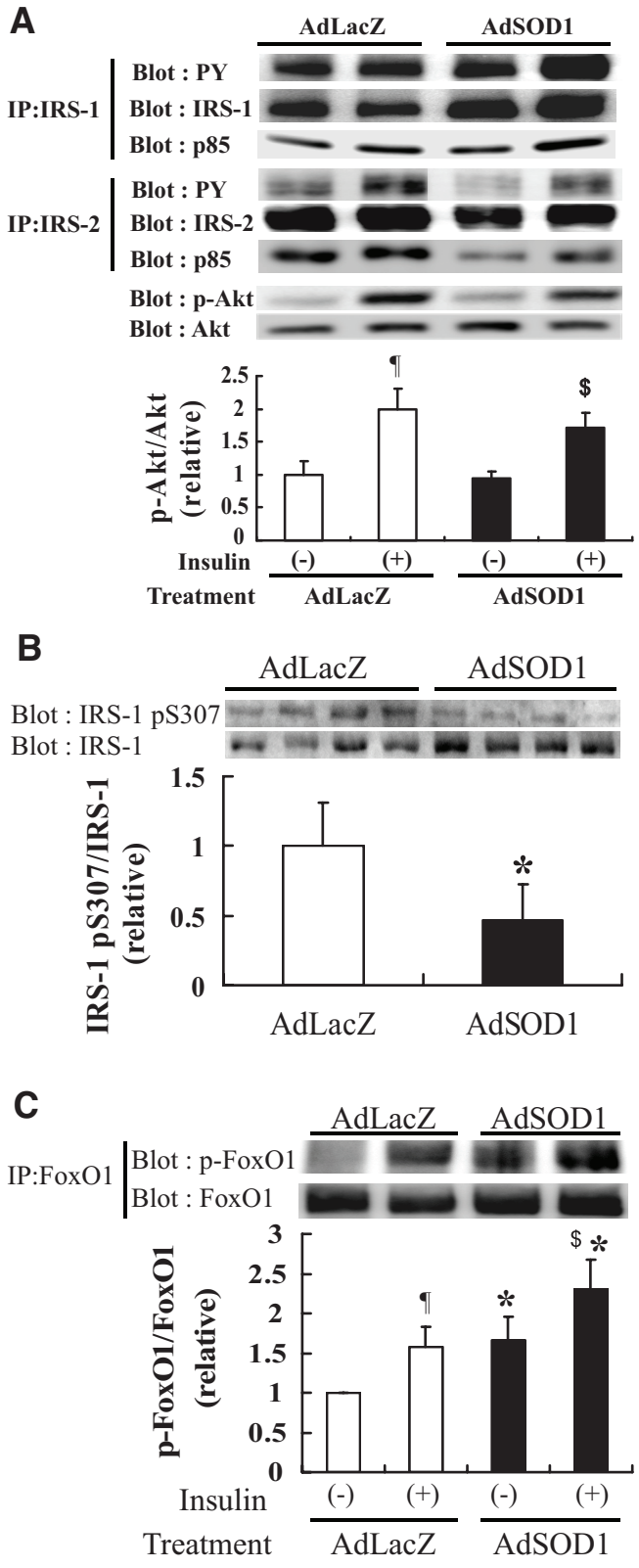


**FIG. 4. Insulin induces phosphorylation and expression of Akt, IRS-1, IRS-2, and Foxo1 in the liver. *A*: At 7 days after treatment of *db/db* mice with AdLacZ or AdSOD1, livers were collected at 5 min after injection of 0.5 units of regular insulin through the inferior vena cava or without the injection of insulin. Whole cell extracts were applied for immunoprecipitation assay using anti–IRS-1 or anti–IRS-2 antibody. The immunoprecipitated samples were applied for Western blotting analysis using the indicated antibodies. Representative results of 3–4 experiments are shown. The *lower panel* showed Akt phosphorylation level in each group. Whole cell extracts from the livers were applied for the detection of insulin-induced Akt phosphorylation (AdLacZ insulin [−], $n = 4$; AdLacZ insulin [+], $n = 7$; AdSOD1 insulin [−], $n = 5$; AdSOD1 insulin [+], $n = 7$). *B*: Liver homogenates were immunoblotted with anti–phosphoIRS-1(Ser$^{307}$) antibody or anti–IRS-1 antibody ($n = 7$ for each treatment). The relative Ser$^{307}$ phosphorylated IRS-1 expression level was expressed by setting the mean density of blots of AdLacZ as 1. *C*: At 7 days after treatment of *db/db* mice with AdLacZ or AdSOD1, livers were collected at 5 min after injection of 0.5 units of regular insulin through the inferior vena cava or without the injection of insulin. Whole cell extracts were applied for immunoprecipitation assay using anti-Foxo1 antibody. The immunoprecipitated samples were applied for Western blotting analysis using anti–phospho-FKHR (Ser$^{256}$) antibody. Representative results of 5–6 experiments are shown. Values are means ± SD. ¶$P < 0.05$ vs. AdLacZ insulin [−] group; \$$P < 0.05$ vs. AdSOD1 insulin [−] group; *$P < 0.05$ vs. corresponding AdLacZ groups.**

genic genes were associated with a significant reduction of mRNA and protein-level PGC-1α, which is the main regulator of the expression of both gluconeogenic genes (16,17). On the other hand, overexpression of SOD1 did not alter the gene expression of glucokinase, the rate-limiting enzyme of glycolysis (Fig. *3*). These data indicate that downregulation of PGC-1α, which is a main regulator of gluconeogenic genes, may play a key role in the improvement of glucose tolerance by the reduction of ROS in *db/db* mice.

**Overexpression of SOD1 increased the phosphorylation of Foxo1 independently of Akt phosphorylation level in the liver.** Insulin suppresses the expression of the PGC-1α gene at least partly through Akt-stimulated phosphorylation of forkhead box class O1 (Foxo1) (18). Thus, we investigated the insulin-signaling transduction pathway in liver of AdLacZ- and AdSOD1-treated *db/db* mice. Although IRS-1 and IRS-2 are both important molecules involved in insulin signaling, the expression of IRS-1 protein in AdSOD1 group was significantly higher, and the expression of IRS-2 protein significantly lower, than that in the AdLacZ group (Fig. 4*A*). We quantitatively confirmed the changes of the expression of these proteins (data not shown). Parallel to the respective expression level, insulin-stimulated tyrosine phosphorylation of IRS-1 was higher and that of IRS-2 was lower in AdSOD1-treated mice than in AdLacZ-treated mice (Fig. 4*A*). Reflecting these changes, the binding affinity to p85, a subunit of PI3 kinase of IRS-1, was higher and that of IRS-2 was lower in AdSOD1-treated mice than in AdLacZ-treated mice (Fig. 4*A*). Probably because the reduced IRS-2 phosphorylation can counteract the increased IRS-1 phosphorylation, insulin-stimulated phosphorylation of Akt might not be eventually affected by overexpression of SOD1 (Fig. 4*A*). IRS-1 is phosphorylated at Ser$^{307}$ residue (5,19,20) by several cytokines; this modification reduces insulin-stimulated tyrosine phosphorylation of IRS-1 and stimulates the degradation of IRS-1 (21,22). Thus, we investigated the effect of reduction of ROS on the phosphorylation of IRS-1 at the Ser$^{307}$ residue. As shown in Fig. 4*B*, phosphorylation of IRS-1 at the Ser$^{307}$ residue was reduced by reduction of ROS. These findings indicate that the increase of insulin-stimulated tyrosine phosphorylation of IRS-1 by the reduction of ROS in liver of *db/db* mice is associated with the decreased phosphorylation of IRS-1 at the Ser$^{307}$ residue.

Finally, we examined the phosphorylation of Foxo1 at Ser$^{256}$. Although no significant change in the phosphorylation level of Akt was observed in association with SOD1 overexpression, the phosphorylation of Foxo1 was significantly augumented by the SOD1 overexpression (Fig. 4*C*). This finding suggests that the phosphorylation of Foxo1 at

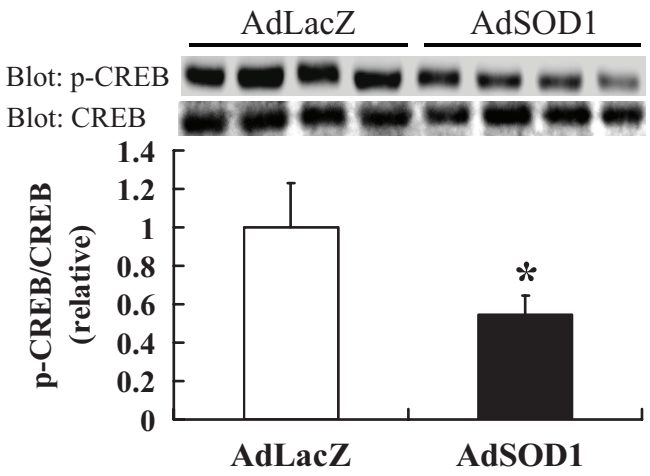


**FIG. 5. Effects of SOD1 overexpression on CREB phosphorylation. *A*: At 7 days after treatment of *db/db* mice with AdLacZ or AdSOD1, livers were collected after overnight fasting. The liver homogenates were immunoblotted with anti–phospho-CREB (*p*-CREB) or anti-CREB antibody ($n = 8$ for each treatment). The relative expression level was calculated by setting the expression level in the liver of mice injected with AdLacZ as 1. Values are means ± SD. *$P < 0.05$ vs. AdLacZ group.**

$Ser^{256}$ may be regulated by oxidative stress, independent of Akt activity.

**Overexpression of SOD1 reduces phosphorylation of CREB.** In response to glucagon, protein kinase A phosphorylates transcription factor CREB at $Ser^{133}$ and increases its transcriptional activity (23), which activates the expression of *PGC-1α* and gluconeogenic genes (16,17). Overexpression of SOD1 reduced phosphorylation of CREB (Fig. 5). This result indicates that the reduced expression of PGC-1α associated with reduction of ROS in liver is accompanied by reduced phosphorylation of CREB.

**ROS induces phosphorylation of CREB and *PGC-1α* gene expression in hepatocytes.** Next, to investigate whether ROS induces the phosphorylation of CREB and, hence, results in activation of PGC1α in hepatocytes, we loaded ROS to a hepatocyte-derived cell line, Huh7 cells, by the addition of xanthine and xanthine oxidase, which generate superoxides. The combination of both compounds augmented CREB phosphorylation, but their effect was suppressed by BHA (a scavenger of free radicals) and MnTBAP (an SOD mimetic material) (Fig. 6*A*). Reflecting the changes in phosphorylation of CREB, ROS augmented PGC-1α expression, and this effect was blocked by pretreatment with BHA or MnTBAP (Fig. 6*B*). These results indicate that high ROS levels activate CREB phosphorylation and result in increased expression of *PGC-1α*.

Previous studies showed that ROS induced phosphorylation and activation of mitogen-activated protein kinases (MAPKs) (5,24–26). In addition, ERK and p38 MAPK regulate the phosphorylation of CREB in hepatocytes and liver (27–29). Thus, we investigated the causal relationship between activation of MAPK and phosphorylation of CREB in the pathogenesis of liver insulin resistance. As shown in Fig. 6*C*, phosphorylation of CREB was higher in *db/db* mice than in *db/m* mice. The increased phosphorylation of CREB was restored by AdSOD1. We measured the phosphorylation state of each MAPK in the same samples. Among MAPKs, only the phosphorylation level of JNK tended to be similar to that of CREB. Next, we investigated the causal relationship between phosphorylation of JNK and CREB in Huh7 cells. As shown in Fig. 6*D*, ROS induced JNK phosphorylation, which was in turn counteracted by the addition of antioxidants. ROS-induced phosphorylation of CREB was also blocked by the addition of JNK-specific inhibitor SP600125 (Fig. 6*E*). In addition, ROS-induced activation of *PGC-1α* was counteracted by SP600125 (Fig. 6*F*). These results indicate that ROS-induced JNK activation is at least in part involved in the pathogenesis of hepatic insulin resistance, through the activation of CREB.

## DISCUSSION

In this study, we investigated the role of ROS on hepatic glucose metabolism in type 2 diabetes. The major findings of the present study were that the ROS–JNK–CREB–PGC-1α pathway is at least in part involved in the pathogenesis of liver insulin resistance.

Hyperglycemia observed in the diabetic state largely depends on increased hepatic glucose production and reduced glucose uptake in peripheral tissues. In particular, increased hepatic gluconeogenesis plays an important role in the pathophysiology of hyperglycemia (30). The regulation of gluconeogenesis predominantly depends on the expression level of gluconeogenic genes such as *PEPCK* and *G6Pase* (31,32). In the present study, overexpression of SOD1 suppressed the expression of gluconeogenic genes. The pyruvate challenge test showed that SOD1 expression in *db/db* mice reduced gluconeogenesis. Thus, whereas we cannot exclude the possibility that the reduction of ROS in liver altered peripheral insulin sensitivity, it is likely that the improvement in glucose level following reduction of ROS in the liver is mainly caused by reduced expression of gluconeogenic genes.

The body weight of AdSOD1-treated mice was higher than that of AdLacZ-treated and PBS-injected mice (Fig. 2*B*), although food intake of AdSOD1-treated mice was comparable with that of AdLacZ-treated and PBS-injected mice (data not shown). Accordingly, the increase in body weight was not due to the increase in appetite associated with the treatment of AdSOD1. In AdSOD1 mice, insulin sensitivity was improved and blood glucose was efficiently reduced. Accordingly, the body-weight gain in AdSOD1-treated mice might be due to the decrease of the urinary glucose excretion and the increase of glucose absorption in insulin-sensitive tissue.

PGC-1α functions as a coactivator of several transcription factors that play critical roles in hepatic glucose metabolism by regulating the expression of gluconeogenic genes (16,17). The expression of PGC-1α is markedly increased in the liver of diabetic rodents (16,17), and inhibition of hepatic PGC-1α expression results in almost complete normalization of fasting glucose level and glucose tolerance in *db/db* mice (33). Furthermore, in nondiabetic rodents, inhibition of PGC-1α reduces hepatic glucose output along with downregulation of *PEPCK* and *G6Pase* expression (33). In the present study, PGC-1α expression was markedly suppressed by SOD1 overexpression, and this seemed to be a key molecular mechanism in the inhibition of gluconeogenesis.

Several studies reported that insulin reduces the expression of PGC-1α in the liver via the inactivation of Foxo1 (18,34–36). Therefore, amelioration of glucose tolerance by reduction of ROS in the liver in *db/db* mice might possibly be due to an increase in insulin signaling. However, the phosphorylation level of Akt, a key signal mole-

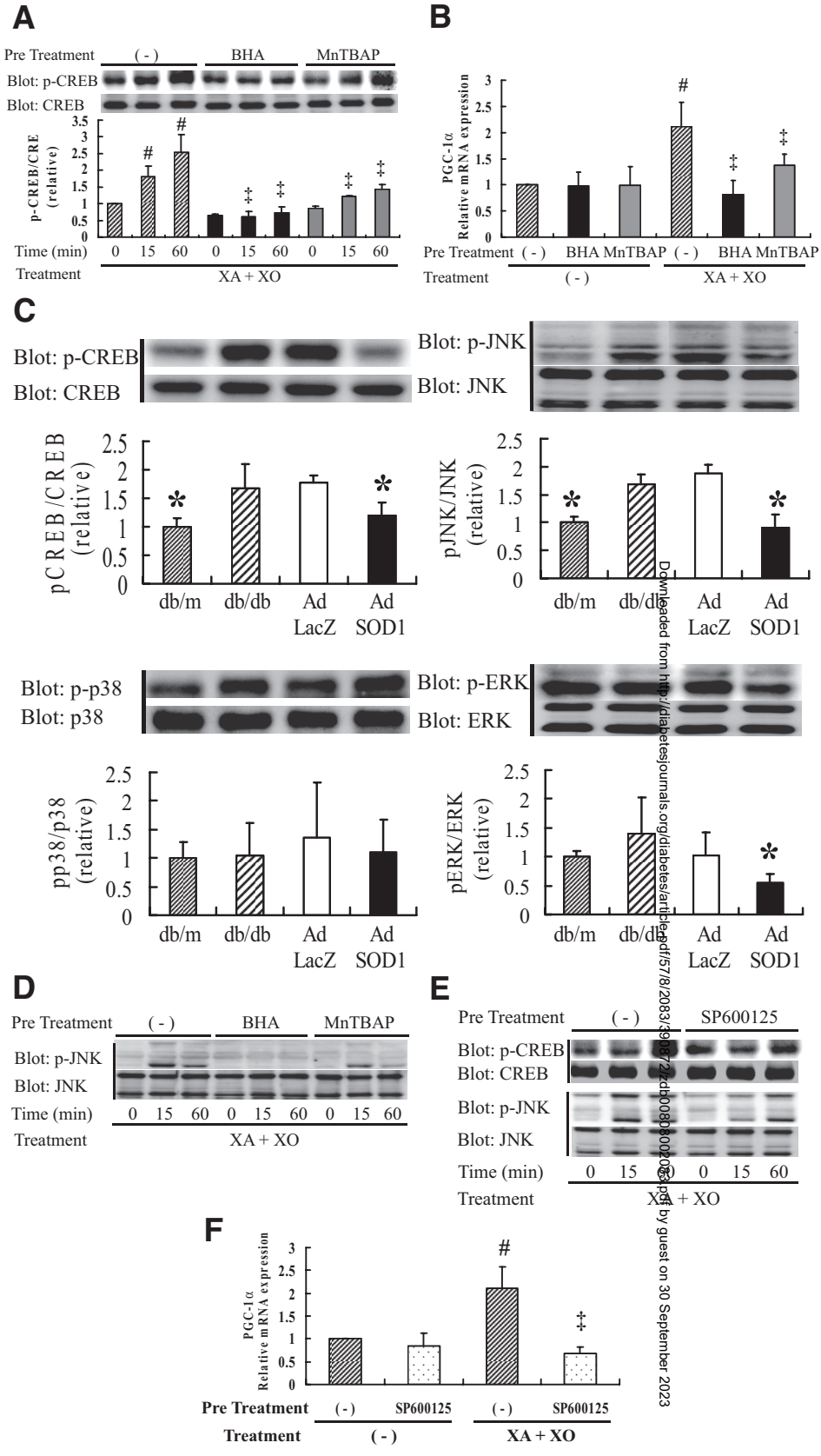




**FIG. 6. ROS induces CREB phosphorylation and *PGC-1α* gene expression in Huh7 cells. *A*: After overnight starvation, Huh7 cells were treated with 400 μmol/l xanthine (XA) and 40 mU/ml xanthine oxidase (XO). The cell extracts were then applied for Western blotting to detect CREB phosphorylation. When antioxidants were used, 400 μmol/l BHA or 400 μmol/l MnTBAP was added to the medium 20 min before treatment with XA and XO. Representative results of 4 experiments were shown. *B*: After overnight starvation, Huh7 cells were treated with 400 μmol/l XA and 40 mU/ml XO for 180 min. Total RNA extracted from each cell was then applied for real-time RT-PCR to quantitate the expression of *PGC-1α*. Values are means ± SD of 4–5 experiments. #$P < 0.05$ vs. pretreatment (−) before XA and XO treatment. ‡$P < 0.05$ vs. pretreatment (−) after XA and XO treatment. *C*: Seven days after intravenous injection of PBS into db/m mice or of PBS, AdLacZ, or AdSOD1 into *db/db* mice, liver was harvested and applied for immunoblotting with the corresponding antibody. Data represent the amounts of phosphorylated protein divided by the amount of the respective protein. The relative expression level was calculated by setting the expression level in liver of db/m mice as 1. Values are means ± SD. *$P < 0.05$ vs. *db/db* and AdLacZ groups. *D*: After overnight starvation, Huh7 cells were treated with 400 μmol/l XA and 40 mU/ml XO. The phosphorylation of JNK was assessed at 15 and 60 min after treatment. The antioxidant (BHA 400 μmol/l or MnTBAP 400 μmol/l) was added at 20 min before the addition of XA and XO. Representative results of four experiments were shown. *E*: Thirty micromolars of SP600125, a JNK-specific inhibitor, were pretreated instead of antioxidants. The phosphorylation of CREB and JNK were then assessed at 15 and 60 min after treatment. Representative results of 4 experiments were shown. *F*: After overnight starvation, Huh7 cells were treated with 400 μmol/l XA and 40 mU/ml XO. Total RNA extracted from each cell was then applied for real-time RT-PCR to quantitate the expression of *PGC-1α*. Thirty μmol/l SP600125 were added 20 min before the addition of XA and XO. Values are means ± SD of 4–5 experiments. #$P < 0.05$ vs. pretreatment (−) before XA and XO treatment. ‡$P < 0.05$ vs. pretreatment (−) after XA and XO treatment for 180 min.**

cule mediating the metabolic actions of insulin, was not altered by reduction of ROS.

Whereas previous studies showed that Akt reduced transactivation of Foxo1 through the phosphorylation of Foxo1 at $Ser^{256}$ (37,38), our data demonstrated that the phosphorylation of Foxo1 at $Ser^{256}$ was augmented by reduction of ROS independently of the insulin signal at Akt phosphorylation level. Very recently, it was reported that the phosphorylation of Foxo1 is regulated by phosphatases such as protein phosphatase 2A and $Ca^{2+}$-dependent

protein phosphatase 2B (calcineurin) (39,40). Both protein phosphatase 2A and calcinurin are known to be activated by ROS (41–46). Therefore, the overexpression of SOD1 may augment the phosphphorylation of Foxo1 by the reduction of phosphatase activity.

While Foxo1 is known as a positive regulator of *PGC-1α*, CREB, which is activated by glucagon and epinephrine, is the main regulator of the *PGC-1α* expression in the liver (16,17). In the present study, we demonstrated that downregulation of PGC-1α expression, elicited by reduced ROS levels in the liver, is accompanied by decreased phosphorylation of CREB in *db/db* mice. These results demonstrate the association of tissue ROS level and phosphorylation level of CREB. A previous study indicated that the expression level of PGC-1α is increased by hydrogen peroxide in mouse fibroblasts and that such an increase was mediated by CREB phosphorylation (47). In the present study, we found that ROS induced phosphorylation of CREB and activation of *PGC-1α* gene expression in Huh7 cells. Thus, ROS-induced CREB phosphorylation may be a common signal pathway in different kinds of cells. Reduction of ROS in liver is a potentially effective strategy to improve insulin resistance.

Previous studies showed that ROS phosphorylates and activates MAPKs in both hepatocytes and liver (5,24–26) and that ERK and p38 MAPK activate CREB. We found that only the phosphorylation of JNK is associated with ROS level in liver among MAPKs. Furthermore, in Huh7 cells, activation of CREB by ROS was suppressed by the JNK inhibitor. Although the mechanism of JNK-mediated CREB phosphorylation should be elucidated, JNK at least partly mediates ROS-induced hepatic insulin resistance through the activation of CREB.

With regard to the effect of ROS on insulin signaling, we investigated tyrosine phosphorylation of IRS-1 and IRS-2. Interestingly, reduction of ROS increased tyrosine phosphorylation of IRS-1 but decreased tyrosine phosphorylation of IRS-2. With regard to the changes in expression and tyrosine phosphorylation of IRS-1, reduction of ROS attenuated phosphorylation of IRS-1 at the $Ser^{307}$ residue. In the present study, reduction of ROS also attenuated JNK activation. JNK reportedly phosphorylates IRS-1 at the $Ser^{307}$ residue (5,19,20) and stimulates the degradation of IRS-1 (21,22). Thus, it is likely that reduction of ROS increases the phosphorylation and expression of IRS-1 through a reduction of JNK activity. With regard to IRS-2, the gene expression is positively regulated by CREB in the liver (48). Thus, reduction of ROS in liver might reduce the gene expression of *IRS-2* by attenuating CREB phosphorylation. Probably because of the opposite changes of insulin signal at IRS-1 and IRS-2, Akt phosphorylation was not affected by reduction of ROS.

In the present study, we used overexpression of SOD1 as a strategy to reduce ROS levels in the liver. As a result of the mitochondrial and cytosolic location of SOD1 in liver (7), overexpression of SOD1 theoretically reduces both mitochondria and cytosolic superoxide. Recently, Imoto et al. (5) reported that ROS derived from mitochondria attenuate insulin signaling in cultured hepatocytes. To determine whether the effect of SOD1 on hepatic insulin resistance is different from that of SOD2 (mitochondrial isoform), we investigated the effect of overexpression of SOD2 in the liver of *db/db* mice using the same strategy as was used for SOD1 treatment in the present study. We found that treatment of *db/db* mice with AdSOD2 reduced blood glucose level and ameliorated glucose tolerance and that the effect was almost similar to overexpression of AdSOD1 (N. Kumashiro and H. Watada, unpublished observations). These results suggest that the reduction of ROS derived from mitochondria may play a key role in the improvement of insulin sensitivity.

In conclusion, our data show that the decreased PGC-1α expression is at least in part involved in the amelioration of liver insulin resistance by the reduction of ROS. The present results suggest that this signal pathway is a potentially suitable therapeutic target for the treatment of type 2 diabetes.

## ACKNOWLEDGMENTS

We thank Dr. David A. Brenner (University of North Carolina), Dr. Michael S. German (University of California San Francisco), and Dr. Ikejima Kenichi (Juntendo University) for providing the indicated materials described in the text. We also thank Naoko Daimaru and Eriko Magoshi for excellent technical assistance.

## REFERENCES

1. Evans JL, Goldfine ID, Maddux BA, Grodsky GM: Oxidative stress and stress-activated signaling pathways: a unifying hypothesis of type 2 diabetes. *Endocr Rev* 23:599–622, 2002
2. Evans JL, Goldfine ID, Maddux BA, Grodsky GM: Are oxidative stress-activated signaling pathways mediators of insulin resistance and beta-cell dysfunction? *Diabetes* 52:1–8, 2003
3. Houstis N, Rosen ED, Lander ES: Reactive oxygen species have a causal role in multiple forms of insulin resistance. *Nature* 440:944–948, 2006
4. Lin Y, Berg AH, Iyengar P, Lam TK, Giacca A, Combs TP, Rajala MW, Du X, Rollman B, Li W, Hawkins M, Barzilai N, Rhodes CJ, Fantus IG, Brownlee M, Scherer PE: The hyperglycemia-induced inflammatory response in adipocytes: the role of reactive oxygen species. *J Biol Chem* 280:4617–4626, 2005
5. Imoto K, Kukidome D, Nishikawa T, Matsuhisa T, Sonoda K, Fujisawa K, Yano M, Motoshima H, Taguchi T, Tsuruzoe K, Matsumura T, Ichijo H, Araki E: Impact of mitochondrial reactive oxygen species and apoptosis signal-regulating kinase 1 on insulin signaling. *Diabetes* 55:1197–1204, 2006
6. Zelko IN, Mariani TJ, Folz RJ: Superoxide dismutase multigene family: a comparison of the CuZn-SOD (SOD1), Mn-SOD (SOD2), and EC-SOD (SOD3) gene structures, evolution, and expression. *Free Radic Biol Med* 33:337–349, 2002
7. Okado-Matsumoto A, Fridovich I: Subcellular distribution of superoxide dismutase (SOD) in rat liver. *J Biol Chem* 276:38388–38393, 2001
8. Lehmann TG, Wheeler MD, Schwabe RF, Connor HD, Schoonhoven R, Bunzendahl H, Brenner DA, Jude Samulski R, Zhong Z, Thurman RG: Gene delivery of Cu/Zn-superoxide dismutase improves graft function after transplantation of fatty livers in the rat. *Hepatology* 32:1255–1264, 2000
9. Minamiyama Y, Takemura S, Toyokuni S, Imaoka S, Funae Y, Hirohashi K, Yoshikawa T, Okada S: CYP3A induction aggravates endotoxemic liver injury via reactive oxygen species in male rats. *Free Radic Biol Med* 37:703–712, 2004
10. Takimoto E, Champion HC, Li M, Ren S, Rodriguez ER, Tavazzi B, Lazzarino G, Paolocci N, Gabrielson KL, Wang Y, Kass DA: Oxidant stress from nitric oxide synthase-3 uncoupling stimulates cardiac pathologic remodeling from chronic pressure load. *J Clin Invest* 115:1221–1231, 2005
11. Tamura Y, Ogihara T, Uchida T, Ikeda F, Kumashiro N, Nomiyama T, Sato F, Hirose T, Tanaka Y, Mochizuki H, Kawamori R, Watada H: Amelioration of glucose tolerance by hepatic inhibition of nuclear factor kappaB in db/db mice. *Diabetologia* 50:131–141, 2007
12. Nomiyama T, Igarashi Y, Taka H, Mineki R, Uchida T, Ogihara T, Choi JB, Uchino H, Tanaka Y, Maegawa H, Kashiwagi A, Murayama K, Kawamori R, Watada H: Reduction of insulin-stimulated glucose uptake by peroxynitrite is concurrent with tyrosine nitration of insulin receptor substrate-1. *Biochem Biophys Res Commun* 320:639–647, 2004
13. Ogihara T, Watada H, Kanno R, Ikeda F, Nomiyama T, Tanaka Y, Nakao A, German MS, Kojima I, Kawamori R: p38 MAPK is involved in activin A- and hepatocyte growth factor-mediated expression of pro-endocrine gene neurogenin 3 in AR42J-B13 cells. *J Biol Chem* 278:21693–21700, 2003
14. Kamata H, Honda S, Maeda S, Chang L, Hirata H, Karin M: Reactive oxygen species promote TNFalpha-induced death and sustained JNK activation by inhibiting MAP kinase phosphatases. *Cell* 120:649–661, 2005

15. Sakon S, Xue X, Takekawa M, Sasazuki T, Okazaki T, Kojima Y, Piao JH, Yagita H, Okumura K, Doi T, Nakano H: NF-kappaB inhibits TNF-induced accumulation of ROS that mediate prolonged MAPK activation and necrotic cell death. *Embo J* 22:3898–3909, 2003
16. Yoon JC, Puigserver P, Chen G, Donovan J, Wu Z, Rhee J, Adelmant G, Stafford J, Kahn CR, Granner DK, Newgard CB, Spiegelman BM: Control of hepatic gluconeogenesis through the transcriptional coactivator PGC-1. *Nature* 413:131–138, 2001
17. Herzig S, Long F, Jhala US, Hedrick S, Quinn R, Bauer A, Rudolph D, Schutz G, Yoon C, Puigserver P, Spiegelman B, Montminy M: CREB regulates hepatic gluconeogenesis through the coactivator PGC-1. *Nature* 413:179–183, 2001
18. Daitoku H, Yamagata K, Matsuzaki H, Hatta M, Fukamizu A: Regulation of PGC-1 promoter activity by protein kinase B and the forkhead transcription factor FKHR. *Diabetes* 52:642–649, 2003
19. Hirosumi J, Tuncman G, Chang L, Gorgun CZ, Uysal KT, Maeda K, Karin M, Hotamisligil GS: A central role for JNK in obesity and insulin resistance. *Nature* 420:333–336, 2002
20. Shoelson SE, Lee J, Goldfine AB: Inflammation and insulin resistance. *J Clin Invest* 116:1793–1801, 2006
21. Greene MW, Sakaue H, Wang L, Alessi DR, Roth RA: Modulation of insulin-stimulated degradation of human insulin receptor substrate-1 by Serine 312 phosphorylation. *J Biol Chem* 278:8199–8211, 2003
22. Hiratani K, Haruta T, Tani A, Kawahara J, Usui I, Kobayashi M: Roles of mTOR and JNK in serine phosphorylation, translocation, and degradation of IRS-1. *Biochem Biophys Res Commun* 335:836–842, 2005
23. Gonzalez GA, Montminy MR: Cyclic AMP stimulates somatostatin gene transcription by phosphorylation of CREB at serine 133. *Cell* 59:675–680, 1989
24. Conde de la Rosa L, Schoemaker MH, Vrenken TE, Buist-Homan M, Havinga R, Jansen PL, Moshage H: Superoxide anions and hydrogen peroxide induce hepatocyte death by different mechanisms: involvement of JNK and ERK MAP kinases. *J Hepatol* 44:918–929, 2006
25. Hsieh CC, Papaconstantinou J: Thioredoxin-ASK1 complex levels regulate ROS-mediated p38 MAPK pathway activity in livers of aged and long-lived Snell dwarf mice. *Faseb J* 20:259–268, 2006
26. Schwabe RF, Brenner DA: Mechanisms of Liver Injury. I. TNF-alpha-induced liver injury: role of IKK, JNK, and ROS pathways. *Am J Physiol Gastrointest Liver Physiol* 290:G583–G589, 2006
27. Qiao L, Han SI, Fang Y, Park JS, Gupta S, Gilfor D, Amorino G, Valerie K, Sealy L, Engelhardt JF, Grant S, Hylemon PB, Dent P: Bile acid regulation of C/EBPbeta, CREB, and c-Jun function, via the extracellular signal-regulated kinase and c-Jun NH2-terminal kinase pathways, modulates the apoptotic response of hepatocytes. *Mol Cell Biol* 23:3052–3066, 2003
28. Cao W, Collins QF, Becker TC, Robidoux J, Lupo EG Jr, Xiong Y, Daniel KW, Floering L, Collins S: p38 Mitogen-activated protein kinase plays a stimulatory role in hepatic gluconeogenesis. *J Biol Chem* 280:42731–42737, 2005
29. Collins QF, Xiong Y, Lupo EG Jr, Liu HY, Cao W: p38 Mitogen-activated protein kinase mediates free fatty acid-induced gluconeogenesis in hepatocytes. *J Biol Chem* 281:24336–24344, 2006
30. Woerle HJ, Szoke E, Meyer C, Dostou JM, Wittlin SD, Gosmanov NR, Welle SL, Gerich JE: Mechanisms for abnormal postprandial glucose metabolism in type 2 diabetes. *Am J Physiol Endocrinol Metab* 290:E67–E77, 2006
31. Sun Y, Liu S, Ferguson S, Wang L, Klepcyk P, Yun JS, Friedman JE: Phosphoenolpyruvate carboxykinase overexpression selectively attenuates insulin signaling and hepatic insulin sensitivity in transgenic mice. *J Biol Chem* 277:23301–23307, 2002
32. Trinh KY, O'Doherty RM, Anderson P, Lange AJ, Newgard CB: Perturbation of fuel homeostasis caused by overexpression of the glucose-6-phosphatase catalytic subunit in liver of normal rats. *J Biol Chem* 273:31615–31620, 1998
33. Koo SH, Satoh H, Herzig S, Lee CH, Hedrick S, Kulkarni R, Evans RM, Olefsky J, Montminy M: PGC-1 promotes insulin resistance in liver through PPAR-alpha-dependent induction of TRB-3. *Nat Med* 10:530–534, 2004
34. Miyake K, Ogawa W, Matsumoto M, Nakamura T, Sakaue H, Kasuga M: Hyperinsulinemia, glucose intolerance, and dyslipidemia induced by acute inhibition of phosphoinositide 3-kinase signaling in the liver. *J Clin Invest* 110:1483–1491, 2002
35. Barthel A, Schmoll D: Novel concepts in insulin regulation of hepatic gluconeogenesis. *Am J Physiol Endocrinol Metab* 285:E685–E692, 2003
36. Zhou XY, Shibusawa N, Naik K, Porras D, Temple K, Ou H, Kaihara K, Roe MW, Brady MJ, Wondisford FE: Insulin regulation of hepatic gluconeogenesis through phosphorylation of CREB-binding protein. *Nat Med* 10:633–637, 2004
37. Zhang X, Gan L, Pan H, Guo S, He X, Olson ST, Mesecar A, Adam S, Unterman TG: Phosphorylation of serine 256 suppresses transactivation by FKHR (FOXO1) by multiple mechanisms: direct and indirect effects on nuclear/cytoplasmic shuttling and DNA binding. *J Biol Chem* 277:45276–45284, 2002
38. Guo S, Rena G, Cichy S, He X, Cohen P, Unterman T: Phosphorylation of serine 256 by protein kinase B disrupts transactivation by FKHR and mediates effects of insulin on insulin-like growth factor-binding protein-1 promoter activity through a conserved insulin response sequence. *J Biol Chem* 274:17184–17192, 1999
39. Yan L, Lavin VA, Moser LR, Cui Q, Kanies C, Yang E: PP2A Regulates the Pro-apoptotic Activity of FOXO1. *J Biol Chem* 283:7411–7420, 2008
40. Shioda N, Han F, Moriguchi S, Fukunaga K: Constitutively active calcineurin mediates delayed neuronal death through Fas-ligand expression via activation of NFAT and FKHR transcriptional activities in mouse brain ischemia. *J Neurochem* 102:1506–1517, 2007
41. Adiga IK, Nair RR: Multiple signaling pathways coordinately mediate reactive oxygen species dependent cardiomyocyte hypertrophy. *Cell Biochem Funct* 2008
42. Rivera A, Maxwell SA: The p53-induced gene-6 (proline oxidase) mediates apoptosis through a calcineurin-dependent pathway. *J Biol Chem* 280: 29346–29354, 2005
43. Maziere C, Morliere P, Massy Z, Kamel S, Louandre C, Conte MA, Maziere JC: Oxidized low-density lipoprotein elicits an intracellular calcium rise and increases the binding activity of the transcription factor NFAT. *Free Radic Biol Med* 38:472–480, 2005
44. Goldbaum O, Richter-Landsberg C: Activation of PP2A-like phosphatase and modulation of tau phosphorylation accompany stress-induced apoptosis in cultured oligodendrocytes. *Glia* 40:271–282, 2002
45. Magenta A, Fasanaro P, Romani S, Di Stefano V, Capogrossi MC, Martelli F: Protein phosphatase 2A subunit PR70 interacts with pRb and mediates its dephosphorylation. *Mol Cell Biol* 28:873–882, 2008
46. Cicchillitti L, Fasanaro P, Biglioli P, Capogrossi MC, Martelli F: Oxidative stress induces protein phosphatase 2A-dependent dephosphorylation of the pocket proteins pRb, p107, and p130. *J Biol Chem* 278:19509–19517, 2003
47. St-Pierre J, Drori S, Uldry M, Silvaggi JM, Rhee J, Jager S, Handschin C, Zheng K, Lin J, Yang W, Simon DK, Bachoo R, Spiegelman BM: Suppression of reactive oxygen species and neurodegeneration by the PGC-1 transcriptional coactivators. *Cell* 127:397–408, 2006
48. Canettieri G, Koo SH, Berdeaux R, Heredia J, Hedrick S, Zhang X, Montminy M: Dual role of the coactivator TORC2 in modulating hepatic glucose output and insulin signaling. *Cell Metab* 2:331–338, 2005